Indocyanine Green Angiography and Optical Coherence Tomography Angiography of Choroidal Neovascularization in Age-Related Macular Degeneration

Chiara M. Eandi,[1] Antonio Ciardella,[2] Mariacristina Parravano,[3] Filippo Missiroli,[4] Camilla Alovisi,[1] Chiara Veronese,[2] Maria C. Morara,[2] Massimo Grossi,[4] Gianni Virgili,[5] and Federico Ricci[4]

[1]Department of Surgical Sciences, Eye Clinic, University of Torino, Italy
[2]Azienda Ospedaliero-Universitaria di Bologna-Policlinico S. Orsola-Malpighi, Unità Operativa Oftalmologia-Ciardella, Bologna, Italy
[3]IRCCS Fondazione G.B. Bietti, Rome, Italy
[4]Department of Surgery and Experimental Medicine, University Tor Vergata, Rome, Italy
[5]Department of Translational Surgery and Medicine, University of Florence, Florence, Italy

Correspondence: Chiara M. Eandi, Department of Surgical Science, Eye Clinic, University of Torino, Torino, Italy, Via Juvarra 19, 10122 Torino, Italy;
ceandi@gmail.com.

Submitted: March 26, 2017
Accepted: June 12, 2017

Citation: Eandi CM, Ciardella A, Parravano M, et al. Indocyanine green angiography and optical coherence tomography angiography of choroidal neovascularization in age-related macular degeneration. *Invest Ophthalmol Vis Sci*. 2017;58:3690–3696. DOI: 10.1167/iovs.17-21941

Purpose. To compare the capability of indocyanine green angiography (ICGA) and optical coherence tomography angiography (OCTA) in detecting choroidal neovascularization (CNV).

Methods. In this prospective study, patients with CNV detected with fluorescein angiography (FA) underwent ICGA and OCTA, spectral domain OCT (SD-OCT), and infrared or fundus color photographs. CNV lesions were outlined on ICGA and OCTA images, and the composition and size of the CNV was documented.

Results. One hundred eighty-two eyes were included. With ICGA, well-defined lesions were observed in 37.9%, partly defined in 44.5%, and undefined in 17% of eyes. On OCTA, well-defined, partly defined, and undefined vessels were observed in 53.8%, 27.5%, and 18.7% of eyes, respectively. There was a good correlation between CNV size measured with the two instruments ($r = 0.84$). However, OCTA underestimated CNV area by about 4.5% (slope coefficient with linear regression: 0.55, 95% confidence interval [CI]: 0.46 to 0.65; intercept: 0.27, 95% CI: −0.2 to 0.56). On ICGA, CNV composition was capillary in 28%, mature in 14.3%, and mixed (capillary and major neovascular complex) in 57.7% of eyes. Similarly, OCTA revealed capillary, mature, and mixed CNV in 28.9%, 15.9%, and 55.5% of eyes, respectively.

Conclusions. OCTA provides the clinician the ability to perform precise structural and vascular assessment of CNV noninvasively. Our study is, to our knowledge, the largest OCTA analysis to date of CNV secondary to neovascular AMD analyzed simultaneously by ICGA and OCTA.

Keywords: indocyanine green angiography, choroidal neovascularization, optical coherence tomography, retina

CNV represents the late stage of AMD. These abnormal blood vessels typically sprout from the choriocapillaris and can penetrate Bruch's membrane into the space beneath the RPE (type 1 CNV) or the subretinal space (type 2 CNV). In some eyes, neovascularization seems to begin from the retinal vessels, induces a pigment epithelium detachment, and finally creates anastomosis with choroidal vasculature (retinal angiomatous proliferation, also called type 3 CNV).[1–3]

Early diagnosis and characterization of choroidal neovascularization (CNV) are crucial for initiating and guiding treatment with an intravitreal inhibitor of VEGF to prevent progressive and invalidating vision loss.[4]

The current gold standard for CNV diagnosis is fluorescein angiography (FA).[5–7] FA uses intravenous fluorescein injection to visualize CNV and to identify the patterns of dye leakage that characterize the different CNV types.[8–10]

Nevertheless, many studies have reported that indocyanine green angiography (ICGA) can improve the ability to detect CNV in patients with neovascular AMD compared to FA alone, particularly when type 1 CNV is present.[11,12] In fact, indocyanine green (ICG) angiograms obtained using both the scanning laser ophthalmoscope and digital video-angiography enabled the visualization of 55% and 61% of CNV, respectively, in cases where the CNV could not be determined with FA.[13–15] Detection of type 2 CNV on ICGA reportedly approaches 100% in patients with neovascular AMD.[16]

A new imaging technology, optical coherence tomography angiography (OCTA), has recently been developed and allows for new insights in the noninvasive visualization of normal and pathologic vascularization. This imaging technique detects erythrocyte movement by comparing sequential OCT B-scans at a given cross section. OCT angiograms are coregistered with OCT B-scans from the same area, allowing for simultaneous visualization of structure and blood flow.[17–20]

OCTA allows for the visualization of both the inner and outer retinal vascular plexi, as well as the choriocapillaris layer,

without the need for dye injection and provides a segmentation of the different layers using the en face OCT modality.[21]

The aim of this study was to compare the capability of ICGA and OCTA in detecting the vascular network in active CNV secondary to wet AMD. We also performed a qualitative analysis of the characteristics and composition of the neovascular lesions.

Methods

This study was approved by the Institutional Review Board of the PTV Foundation, and informed consent was obtained from patients before examination. The research adhered to the tenets of the Declaration of Helsinki.

In this prospective study, subjects were enrolled between February 2015 and June 2016 at four different retina centers in Italy, including the Retina Service of the PTV Foundation in Rome; the University Eye Clinic in Torino, the Sant'Orsola Hospital in Bologna, and the IRCCS Bietti Eye Foundation in Rome.

Patients affected by AMD with active CNV detected with FA were further studied with ICGA (Spectralis; Heidelberg Engineering, Heidelberg, Germany) and OCTA (AngioVue Imaging System; Optovue, Inc., Fremont, CA, USA), spectral-domain (SD-OCT) (Spectralis; Heidelberg Engineering), and infrared (IR) images or fundus color photographs (FP) (Topcon TRC IA; Topcon, Tokyo, Japan). Both naïve patients and patients with recurrences were included. The exams were performed on the same day or within 1 week. Best-corrected visual acuity (BCVA) was measured with Early Treatment Diabetic Retinopathy Study charts before dilation of the pupils.

The AngioVue imaging system used to obtain OCTA images has an A-scan rate of 70,000 scans per second, using a light source centered on 840 nm and a bandwidth of 50 nm. Each OCTA volume contains 304 × 304 A-scans with two consecutive B-scans captured at each fixed position before proceeding to the next sampling location. Split-spectrum amplitude-decorrelation angiography (SSADA) was used to extract the OCTA information. Each OCTA volume is acquired in 3 seconds, and two orthogonal OCTA volumes were acquired in order to perform motion correction to minimize motion artifacts arising from microsaccades and fixation changes. Angiography information displayed is the average of the decorrelation values when viewed perpendicularly through the thickness being evaluated.

We used a research version of the AngioVue OCTA software.[21,22]

Orthogonal registration and merging of two consecutive scan volumes were used to obtain 3 × 3-mm and 6 × 6-mm OCTA volumes of both eyes of each patient. Both 3 × 3-mm and 6 × 6-mm OCTA volumes used a 304 × 304 scanning pattern. Standard OCT B-scans were performed to confirm the intraretinal or subretinal fluid presence confirming the lesion activity.

The OCTA software was used to delineate a region of interest with a slab thickness of 30 μm. The software did not allow modification of the segmentation curve of the inner or outer retina; it only allowed moving the original automated segmentation lines up or down. We used the "outer retina" segmentation, which in the software is by default automatically based on the contour of the Bruch's membrane. Therefore, we chose to locate the outer boundary directly anterior to Bruch's membrane to minimize the amount of choroidal vasculature included in the slab. The inner boundary was set to contain the innermost region suspicious of a CNV, as demonstrated in the B-scan.

The built-in automatic artifact removal tool was used to remove retinal vessel shadowing from the en face flow image. This function allowed us to subtract vessels located above the inner border (inner retina vessels) from the outer retina OCTA image.

The 3 × 3-mm OCTA images were used primarily to evaluate each eye. In cases where the 3 × 3-mm OCTA image showed a CNV that extended beyond the image border, a 6 × 6-mm OCTA image was used so that the entire borders of the CNV could be evaluated. There were no lesions extended beyond the 6 × 6 area. In order to measure the CNV lesion size on OCTA, we used the imaging system provided by AngioVue software (AngioVue, RTVue XR Avanti; Optovue, Inc.), by selecting "Flow Area" function.

ICG angiograms were acquired (Spectralis) using a 30-degree field and art mode of 15 images. Early-to-mid-phase ICG angiograms of the detailed vascular structure of the CNV were screened, and the best angiograms were used for image analysis. To measure the CNV lesion size on ICGA we used the area-measuring software provided by Spectralis.

Appearance of CNV on both ICGA and OCTA images was classified as well-defined (the CNV network is entirely visible in all its extension, and all the borders are evident); partly defined (the CNV network is not visible in all its extension and some borders are missing); or undefined (it is not possible to differentiate the CNV network from the choroidal background signal).

When detectable either on ICGA or OCTA, capillary and arteriovenular components of CNV were identified in order to classify the lesion as follows:

1. Capillary (typically spoke wheel or sea fan–shaped lesions composed by tiny curled vessels with anastomotic connections at the CNV border)
2. Mixed (capillary plus mature vessels)
3. Mature (arteriovenular or major neovascular complex [MNC] made by large-diameter dendritic trunks with a negligible or absent capillary component)
4. RAP (focal anastomotic neovascular complex arising from the deep retina capillary plexus)
5. Polypoidal choroidal vasculopathy (PCV; presence of single or multiple focal nodular ectatic lesions at the edge of a sub-RPE neovessel network).

Subretinal (SRF) and intraretinal fluid (IRF) was determined to be present or absent using the correlated OCT B-scans. SD-OCT B-scans were also analyzed to detect the presence of fibrovascular pigment epithelium detachment (PED) or serous PED.

FP or IR photographs were evaluated for the presence of intra- or subretinal hemorrhages and fibrosis.

All the images (OCTA, B-scan SD-OCT, FA, ICGA, FP, and IR) were evaluated independently by two trained readers (CME, MP) from the University Eye Clinic of Torino and the IRCCS Bietti Eye Foundation, respectively, to confirm the diagnosis and to define the characteristics of the CNV. The readers were masked, and in particular, they first evaluated the B-scan SD-OCT, FA, ICGA, FP, and IR. OCTA images were evaluated separately without knowing the corresponding ICGA in order to decrease possible bias. In case of discordance the measurements were reevaluated by a third retinal specialist (FR).

In order to compare the performance of ICGA and OCTA in defining CNV borders (three categories), we used asymptotic symmetry and marginal homogeneity tests, which are suitable for K × K tables where there is a one-to-one matching of cases classified by means of ordered variables. We used ordinal logistic regression to investigate covariates associated with

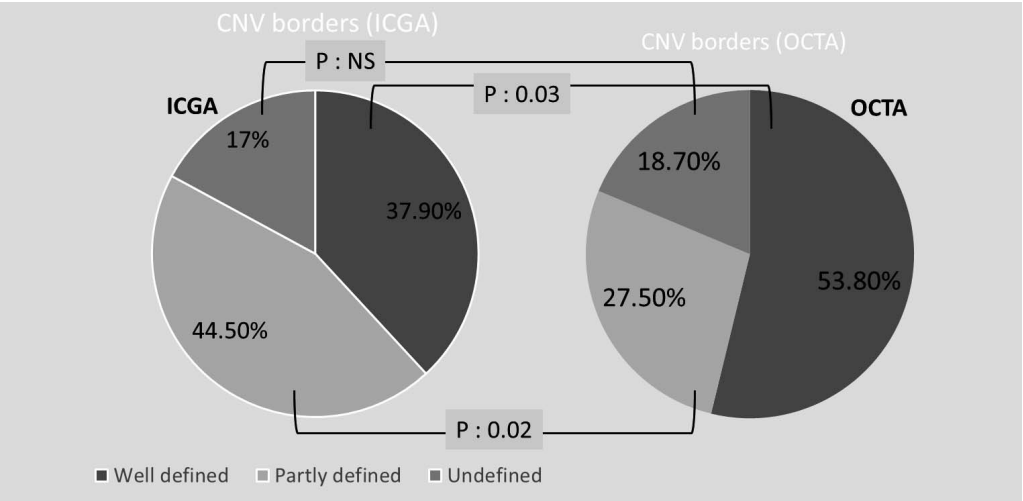

FIGURE 1. CNV borders defined by ICGA (*left*) and OCTA (*right*). The figure shows agreement of ICGA and OCTA in defining CNV borders in 182 patients. More than half of the CNVs were well-defined with OCTA (53.80%), as compared to one-third with ICGA (37.90%) ($P = 0.03$). Partly defined CNVs were identified mostly with ICGA (44.50%) rather than with OCTA (27.50%) ($P = 0.02$). No statistical significant difference was found for undefined CNV with ICGA and OCTA (17% and 18.70%, respectively). NS, nonstatistically significant.

border definition, and we used a χ^2 test to compare frequencies in subgroups of unordered categories.

We used linear regression to investigate the need for calibration of lesion size with OCTA as compared to ICGA. We compared a number of clinical characteristics in capillary OCTA lesions versus other types of lesions using a χ^2 test.

RESULTS

Study Population

One hundred eighty-two eyes of 182 consecutive patients with wet AMD were enrolled in this study. All were Caucasian with a mean age of 74 ± 3.8 years (range, 58–89). There were 111 (61%) women. Each patient underwent BCVA examination, FP or IR photograph, FA, ICGA, SD-OCT, and OCTA examination on the same day or within 1 week. No adverse effects related to the procedures (i.e., dye injection) were reported.

One hundred five of 182 (58%) eyes were naïve CNV, while 77 of 182 (42%) eyes presented recurrent CNV with active leakage on FA or IRF or SRF on B-scan SD-OCT. Mean BCVA was 20/50 Snellen equivalent (range 20/20–20/400). Hemorrhages and fibrosis were present in 45 of 182 (24.7%) and 61 of 182 (33.5%) eyes, respectively. On FA, most of the CNV were type 1 (73%), followed by type 2 (27%). ICGA confirmed type 3 or RAP and PCV lesions in 14 (7.7%) and 12 (6.6%) eyes, respectively. B-scan SD-OCT showed the presence of SRF and IRF in 122 of 182 (67%) and 75 of 182 (41.2%) eyes, respectively. Fibrovascular PED was detected in 102 of 182 (56%) eyes and serous PED in 53 of 182 (29.1%) eyes.

Definition of CNV Borders

When analyzed with ICGA, well-defined lesions were observed in 37.9% (69/182) of eyes, partly defined in 44.5% (81/182) of eyes, and undefined in 17% (32/182) of eyes. On OCTA images, well-defined, partly defined, and undefined vessels were observed in 53.8% (98/182), 27.5% (50/182), and 18.7% (34/182) of eyes, respectively. The intra/subretinal fluid was minimal or absent in all eyes and could not influence the OCTA flow images. The PCV lesions identified on ICGA were not visible on the choroidal background and therefore were classified as "undefined" on OCTA.

Figure 1 shows the agreement of ICGA and OCTA in defining CNV borders in 182 patients with complete data. More than half of the CNVs were well-defined with OCTA, as compared to one-third with ICGA. Overall, there was only moderate agreement between the two techniques ($\kappa = 0.40$). Both the symmetry test and the marginal homogeneity test were highly significant ($P < 0.01$), thus indicating a difference in the degree of border definition between the two tests. Specifically, the largest contribution to the symmetry χ^2 was given by the fact that CNVs that were well-defined in OCTA versus partly defined in ICGA were about four times that of those well-defined in ICGA and partly defined in OCTA. Similar ratios of asymmetry were found in other matched cells.

Asymmetry remained highly significant when the analysis was restricted to 133 type 1 CNVs. A similar subanalysis was not possible on 46 type 2 CNVs, 14 type 3 CNVs, and 12 PCVs due to the limited sample size.

CNV Size

Figure 2 shows the relationship between CNV size (area in square millimeters) with OCTA as compared to ICGA, including lesions that were well-defined with both techniques ($n = 59$). There was a good correlation between CNV size measured with the two instruments ($r = 0.84$). However, as seen in Figure 2, OCTA underestimated CNV area by about 4.5% (slope coefficient with linear regression: 0.55, 95% CI: 0.46 to 0.65; intercept: 0.27, 95% CI: –0.2 to 0.56), suggesting the need for a calibration formula. No difference in size by OCTA CNV type was detected using a regression model ($P = 0.507$).

Characteristics of CNV Lesions

When analyzed with ICGA, CNV composition results were capillary in 28% (51/182) of eyes, mature in 14.3% (26/182) of eyes, and mixed (capillary and MNC) in 57.7% (105/182) of eyes. OCTA images revealed capillary CNV in 28.9% (52/182) of eyes, mature in 15.9% (29/182) of eyes, and mixed in 55.5% (101/182) of eyes.

We explored the characteristics of different CNV types in OCTA, considering clinical, FA, and OCTA margin definition, after excluding type 3 CNVs ($n = 14$). For this purpose, we compared capillary CNVs to other types, thus trying to

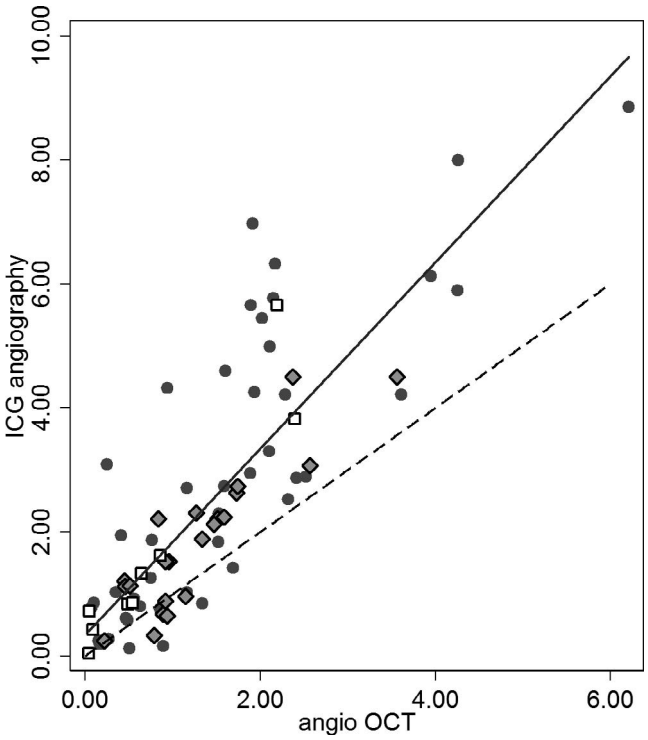

Figure 2. Relationship between CNV size with OCTA as compared to ICGA. There was a good correlation between CNV size (area in square millimeters) measured with the two instruments ($r = 0.84$). However, OCTA underestimated CNV area by about 4.5% (slope coefficient with linear regression: 0.55, 95% CI: 0.46 to 0.65; intercept: 0.27, 95% CI: −0.2 to 0.56). No difference in size by OCTA CNV type was detected ($P = 0.507$). Different marker symbols are displayed for OCTA CNV subtypes: capillary (*dark circle*), capillary + MNC (*gray diamond*), mixed (*empty square*); the *dotted line* presents the equivalence line, where CNV size values (in square millimeters) with ICGA and OCTA are equivalent. The *solid line* presents the linear fit as predicted in a regression model and shows that ICGA overestimates size with respect to OCTA.

characterize lesions that did not have mature choroidal vessels on OCTA (Table). Compared to other CNV types, capillary lesions were more likely to be type 2 CNV and to have well-defined OCTA margins, while they were less likely to show fibrovascular PED (Figs. 3, 4).

Factors Associated With Border Definition With ICGA and OCTA

We explored the characteristics associated with well-defined borders separately for ICGA and OCTA. Results were consistent using both forward and backward ordinal logistic regression. We found that better defined borders with ICGA were more often found in naïve (odds ratio [OR] 2.1, $P = 0.023$) and type 2 (OR 2.8, $P = 0.003$) lesions and less often in lesions showing staining with borderline statistical significance (OR 0.52, $P = 0.065$). On the other hand, better defined lesions in OCTA were more likely type 2 CNV (OR 2.6, $P = 0.010$) and capillary CNV rather than mixed CNV (OR 3.0, $P = 0.003$).

Discussion

Presented in this article is a large qualitative study that investigated OCTA imaging using a commercially available OCTA system.

Table. Comparison of Morphologic CNV Characteristics, as Assessed With Multimodal Imaging, by OCTA Subtype

Morphologic Characteristics	Capillary, % $n = 128$	MNC or Mixed, % $n = 51$	*P* Value
Type 2 (vs. others)	39	20%	0.003*
Leakage (FA)	88	79	0.144
Staining (FA)	19	31	0.115
Fibrovascular PED	33	65	<0.001*
Serous PED	23	32	0.256
Blood	29	23	0.415
Fibrosis	25	37	0.124
Subretinal fluid	63	68	0.517
Intraretinal fluid	50	38	0.128
Well-defined OCTA margins	75	45	<0.001*

Distinct morphologic features are compared between capillary lesions and other choroidal neovascular membranes that did not have mature choroidal vessels on OCTA. Compared to other CNV types, capillary lesions were more likely to be type 2 CNV and to have well-defined OCTA margins, while they were less likely to show PED.

* Statistically significant ($P < 0.01$).

While FA remains the gold standard in the initial diagnosis of neovascular AMD,[7,23,24] and while SD-OCT has become an indispensable technique in the management of wet AMD due to its capability to assess the presence of intra/subretinal fluid accumulation,[25] ICGA is useful in defining the subtypes and the exact area of CNV.[11] However, ICGA is invasive, and the dye injection, although considered safe, has risks ranging from discomfort and nausea to, in rare cases, anaphylaxis. In addition, the technique is expensive (the best results are achievable only by scanning laser devices) and time-consuming, requiring up to 10 minutes of imaging time, which can limit its routine use in a busy clinical setting.[26,27]

The OCTA is a noninvasive, rapid technique for imaging CNV via semiautomated segmentation of the outer retina and subretinal or sub-RPE space from a volumetric OCTA data set. Moreover, corresponding OCT B-scans obtained concurrently were useful in identifying subretinal fluid and other anatomic nonvascular features that were also relevant in the diagnosis of CNV and disease activity.

OCT angiography provides a unique opportunity to directly visualize and study neovascular membranes and their microvascular details in both type 1 and type 2 AMD complexes, which are otherwise only visible with ICGA.[28]

We were able to collect 182 eyes with AMD and type 1, type 2, type 3, or PCV neovascularization and to carefully study, characterize, and analyze the borders, the size, and the morphology of the vascular complex with different imaging modalities.

In this study we demonstrated a moderate agreement between ICGA and OCTA in defining CNV borders, with higher percentage of well-defined lesion borders detected by OCTA. This might be due primarily to the nature of the CNV lesion. In fact, almost two-thirds of the lesions were type 1 CNV located below the RPE. The amount of subretinal fluid was minimal and less likely to influence the border definition on OCTA. The use of SD-OCTA might represent another factor influencing the quality of imaging of CNV mostly when compared to swept-source OCTA (SS-OCTA).

Previous studies showed similar results when comparing OCTA with FA. In particular, de Carlo et al.[20] reported a sensitivity and specificity of CNV detection by OCTA of 50% and 91%, respectively. Also Kuehlewein et al.[28] reported a large series of type1 CNV detected by OCTA. They were able to

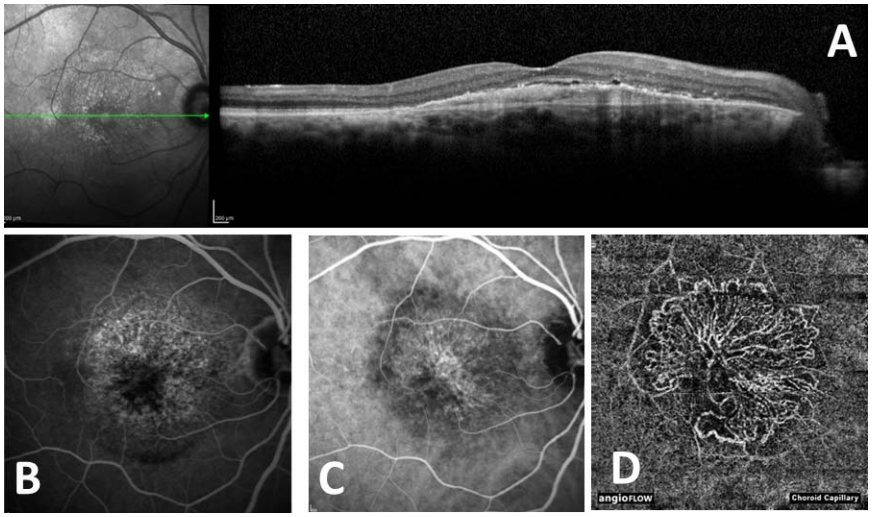

FIGURE 3. Type 1 CNV in the right eye of an 81-year-old man. (**A**) OCT B-scan and corresponding IR image shows a subfoveal vascularized PED with small subretinal fluid. (**B**) FA evidences an irregular iperfluorescence in the macular area, that (**C**) corresponds to CNV evident on ICGA. (**D**) OCTA demonstrates the CNV with well-defined borders and mixed composition.

noninvasively assess the structure and vascular composition of neovascular membrane secondary to wet AMD.

Other studies, using different devices and different decorrelation algorithms (SD-OCT or swept-source OCT, Spectralis OCTA prototype) reported that the sensitivity of the OCTA in detecting choroidal neovascular lesions ranged from 50% to 100%.[20,21,25,29]

In particular, Jia et al.[21] reported five cases of CNV and compared them with normal eyes using OCTA from a prototype SS-OCT. Their prototype system operated at 100,000 A-scans per second to acquire 200 × 200 A-scans in 3.5 seconds. Orthogonal registration and merging of four scans were then used to create 3 × 3-mm OCTA images.

The AngioVue system used in this study operates at 70,000 A-scans per second to obtain 304 × 304 A-scans in 2.6 seconds, merging and registering two consecutive scans to achieve 3 × 3-mm or 6 × 6-mm OCTA images. Therefore, the AngioVue system with the SSADA algorithm, although using a lower scanning speed, allows for shorter imaging time than the SS-OCT prototype thanks to the lower number (two) of repeat B-scans required at each location.

A recent study using the Spectralis prototype reported the correspondence between OCTA and traditional multimodal imaging techniques ranged between 94.9% and 90.5% concerning treatment decision in a series of eyes with CNV.[25]

Our findings regarding the size of the CNV demonstrated a good correlation between the areas measured with the two instruments, despite the need for a calibration formula. In fact, ICGA overestimated the CNV area by 30%, probably due to the different acquisition field of 30 × 30 degrees and 3 × 3 mm for the ICGA and OCTA, respectively, as well as the different software used to measure the CNV size. A recent paper compared the measurement of type 1 CNV with ICGA and OCTA. Costanzo et al.[30] reported that the lesion size in OCTA

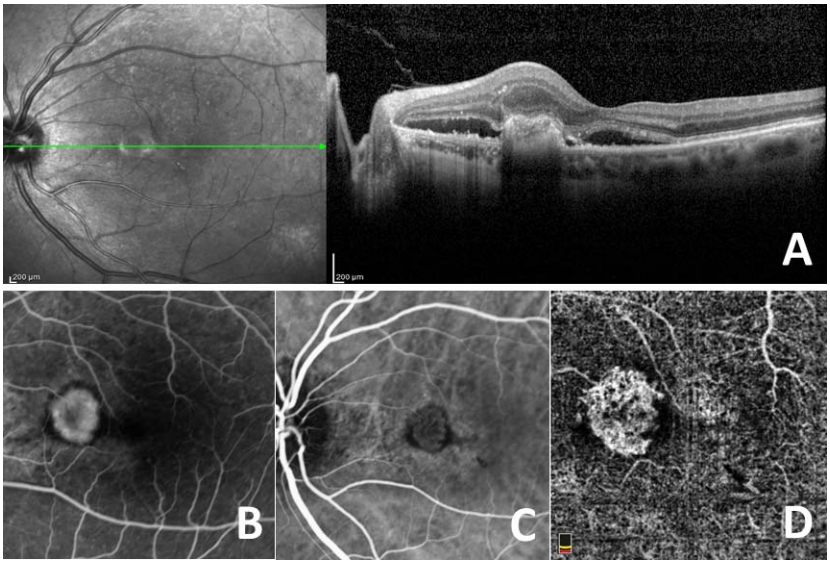

FIGURE 4. Type 2 CNV in the left eye of a 75-year-old man. (**A**) OCT B-scan and corresponding IR image shows a juxtafoveal iperreflective area and adjacent subretinal fluid. (**B**) FA evidences a juxtafoveal CNV with well-defined borders. (**C**) Corresponding ICGA confirms the presence of the well-defined CNV. (**D**) OCTA demonstrates the capillary CNV with well-defined borders.

measured in the choriocapillaris segmentation is significantly smaller than the lesion size measured in both intermediate and late frames of ICGA. Moreover, recent papers reported different CNV size when measured with SS-OCTA or SD-OCTA and compared to ICGA. In particular, Roisman et al.[31] demonstrated that CNV size on SS-OCTA images were comparable to the size of the plaque identified on ICGA, while Miller et al.[32] showed a larger CNV area when imaged with SS-OCTA than with SD-OCTA.

Analysis of CNV composition revealed a similar capability to detect capillary pattern, as well as mixed and mature vessels with OCTA and ICGA.

Our findings regarding the morphology of the membrane are similar to those described by Kuehlewein et al.[28] in type 1 CNV. They reported two patterns of vascular complex, the "medusa-like" and the "sea fan–like" complexes, both characterized by a large main central vessel trunk. This finding of a feeder vessel has also been investigated by Jia and associates[21] using a prototype of SS-OCT angiography and is likely a characteristic of more chronic and mature neovascular complexes associated with chronic PED and longstanding anti-VEGF therapy.[28]

We believe that an important clinical application of OCTA is its ability to noninvasively visualize the extension and morphology of CNVs in order to follow and potentially predict the response to anti-VEGF treatment. There are already some reports describing the neovascular network changes. In particular, Spaide[33] analyzed OCTA images in patients undergoing treatment with anti-VEGF agents. The author describes CNVs identifiable on OCTA that have large trunks and prominent peripheral anastomoses. He attributes this to chronic pruning of small neovascular capillaries by repeated treatment with anti-VEGF agents, resulting in arteriogenesis of the remaining vessels.[34] Also, Muakkassa et al.[34] reported a decrease of CNV greatest linear dimension and CNV area as measured on the OCTA angiogram in a small number of treatment- naïve patients after treatment with intravitreal bevacizumab.

OCT angiography is a promising imaging modality that will likely limit the need for invasive FA and ICGA in the setting of neovascular AMD and may guide evaluation and treatment of this disorder in the future, although technical limitations are still considerable and need to be addressed. In particular, because OCTA technology relies on the detection of blood flow and movement, any movement by the patient will cause significant artifact and deterioration of image quality. Projection artifact is another limitation of this technology, making it sometimes difficult to distinguish normal physiological vessels from pathologic ones. The software does provide a "remove artifacts" function, which can subtract projection artifact from superficial vessels, but this also causes some loss of signal of pathologic blood vessels. Finally, not all neovascular complexes are visualized because of imprecision in slab segmentation, which requires careful control of the depth and thickness of the slab to more precisely identify the neovascular membrane. However, sometimes segmentation to remove choriocapillaris was not possible using the current automated prototype software because the user was unable to manually correct the shape of the automatically detected curvature lines delineating the region of interest. In the future, adding the ability to correct the segmentation curvature manually could further facilitate the accuracy of the AngioVue OCTA software.

Furthermore, because it relies on changes between two consecutive B-scans, OCTA detects only flow that is higher than a minimal threshold, the slowest detectable flow, which is determined by the time between the two sequential OCT B-scans. Slow-flow lesions that have flow of less than the slowest detectable flow therefore would not be visualized using this imaging technique. Increasing the time between consecutive OCT B-scans could allow for increased flow detection but would offer a trade-off of increased movement artifact.

In summary, OCT angiography provides the clinician the ability to perform precise structural and vascular assessment of CNV noninvasively.

To our knowledge, our study is the largest OCT angiography analysis to date of neovascular membranes secondary to neovascular AMD analyzed simultaneously with ICGA and OCTA. It presents, of course, some limitations. In particular, the number of PCV and type 3 lesions was too small to perform statistical analysis. Moreover, the field of ICGA and OCTA images was different, as well as the software used to measure the CNV lesion, resulting in an overestimation of the lesion size with ICGA compared to OCTA.

Future studies with more varied patient demographics and larger sample sizes for higher-powered sensitivity and specificity determinations are necessary to evaluate the robustness of this technique with various types of CNV.

Acknowledgments

Disclosure: **C.M. Eandi**, None; **A. Ciardella**, None; **M. Parravano**, None; **F. Missiroli**, None; **C. Alovisi**, None; **C. Veronese**, None; **M.C. Morara**, None; **M. Grossi**, None; **G. Virgili**, None; **F. Ricci**, None

References

1. Ferrara D, Mohler KJ, Waheed N, et al. En-face enhanced depth swept-source optical coherence tomography features of chronic central serous chorioretinopathy. *Ophthalmology*. 2014;121:719–726.
2. Ambati J, Ambati BK, Yoo SH, et al. Age-related macular degeneration: etiology, pathogenesis, and therapeutic strategies. *Surv Ophthalmol*. 2003;48:257–293.
3. Yannuzzi LA, Negrao S, Lida T, et al. Retinal angiomatous proliferation in age-related macular degeneration. *Retina*. 2001;21:416–434.
4. Jia Y, Bailey ST, Wilson DJ, et al. Quantitative optical coherence tomography angiography of choroidal neovascularization in age-related macular degeneration. *Ophthalmology*. 2014;121:1435–1444.
5. Do DV, Gower EW, Cassard SD, et al. Detection of new-onset choroidal neovascularization using optical coherence tomography: the AMD DOC study. *Ophthalmology*. 2012;119:77–78.
6. Kotsolis AI, Killian FA, Ladas ID, Yannuzzi LA. Fluorescein angiography and optical coherence tomography concordance for choroidal neovascularization in multifocal choroiditis. *Br J Ophthalmol*. 2010;94:1506–1508.
7. Do DV. Detection of new-onset choroidal neovascularization. *Curr Opin Ophthalmol*. 2013;24:224–227.
8. Ryan SJ, Sadda SR, Hinton DR, et al. Age-related macular degeneration. In: Ryan SJ, Sadda SR, Hinton DR, eds. *Retina*. 5th ed. Vol. 1. London: Elsevier Saunders; 2013:1150–1182.
9. Shah SM, Tatlipinar S, Quinlan E, et al. Dynamic and quantitative analysis of choroidal neovascularization by fluorescein angiography. *Invest Ophthalmol Vis Sci*. 2006; 47:5460–5468.
10. Sulzbacher F, Kiss C, Munk M, et al. Diagnostic evaluation of type 2 (classic) choroidal neovascularization: optical coherence tomography, indocyanine green angiography, and fluorescein angiography. *Ophthalmology*. 2011;152:799–806.
11. Guyer DR, Yannuzzi LA, Slakter J, Al E. Diagnostic indocyanine green angiography videoangiography. In: Ryan SJ, Schachat AP, eds. *Retina*. Vol. 3. St. Louis, MO; Mosby; 2001: 943–966.

12. Koh AHC, Chen LJ, Chen SJ, et al. Polypoidal choroidal vasculopathy. Evidence-based guidelines for clinical diagnosis and treatment. *Retina*. 2013;33:686–716.
13. Watzke RC, Klein ML, Hiner CJ, et al. A comparison of stereoscopic fluorescein angiography with indocyanine green videoangiography in age-related macular degeneration. *Ophthalmology*. 2000;107:1601–1606
14. Schneider U, Kuck H, Inhoffen W, Kreissig I. Indocyanine green angiographically well-defined choroidal neovascularization: angiographic patterns obtained using the scanning laser ophthalmoscope. *Ger J Ophthalmol*. 1995;4:67–74.
15. Wolf S, Knabben H, Krombach G, et al. Indocyanine-green angiography in patients with occult choroidal neovascularization. *Ger J Ophthalmol*. 1996;5:251–256.
16. Semoun O, Guigui B, Tick S, et al. Infrared features of classic choroidal neovascularisation in exudative age-related macular degeneration. *Br J Ophthalmol*. 2009;93:182–185.
17. Kim DY, Finger J, Zawadzki RJ, et al. Optical imaging of the chorioretinal vasculature in the living human eye. *Proc Natl Acad Sci U S A*. 2013;110:14354–14359.
18. Choi W, Mohler KJ, Potsaid B, et al. Choriocapillaris and choroidal microvasculature imaging with ultrahigh speed OCT angiography. *PLoS One*. 2013;8:e81499.
19. Schwartz DM, Fingler J, Kim DY, et al. Phase-variance optical coherence tomography: a technique for noninvasive angiography. *Ophthalmology*. 2014;121:180–187.
20. De Carlo TE, Bonini Filho MA, Chin AT, et al. Spectral-domain optical coherence tomography angiography of choroidal neovascularization. *Ophthalmology*. 2015;122:1228–1238.
21. Jia Y, Bailey ST, Wilson DJ, et al. Quantitative optical coherence tomography angiography of choroidal neovascularization in age-related macular degeneration. *Ophthalmology*. 2014;121:1435–1444.
22. Tokayer J, Jia Y, Dhalla AH, Huang D. Blood flow velocity quantification using split-spectrum amplitude-decorrelation angiography with optical coherence tomography. *Biomed Opt Express*. 2013;4:1909–1924.
23. Gass JD. Pathogenesis of disciform detachment of the neuroepithelium. *Am J Ophthalmol*. 1967;63:S1–S139.
24. Hyvärinen L, Flower RW. Indocyanine green fluorescence angiography. *Acta Ophthalmol*. 1980;58:528–538.
25. Coscas GJ, Lupidi M, Coscas F, Cagini C, Souied EH. Optical coherence tomography angiography versus traditional multimodal imaging in assessing the activity of exudative age-related macular degeneration: a new diagnostic challenge. *Retina*. 2015;35:2219–2228.
26. Kwiterovich KA, Maguire MG, Murphy RP, et al. Frequency of adverse systemic reactions after fluorescein angiography. Results of a prospective study. *Ophthalmology*. 1991;98:1139–1144.
27. Lopez-Saez MP, Ordoqui E, Tornero P, et al. Fluorescein induced allergic reaction. *Ann Allergy Asthma Immunol*. 1998;81:428–430.
28. Kuehlewein L, Bansal M, Lenis TL, et al. Optical coherence tomography angiography of type 1 neovascularization in age-related macular degeneration. *Am J Ophthalmol*. 2015;160:739–748.
29. Moult E, Choi W, Waheed NK, et al. Ultrahigh-speed swept-source OCT angiography in exudative AMD. *Ophthalmic Surg Lasers Imaging Retina*. 2014;45:496–505.
30. Costanzo E, Miere A, Querques G, et al. Type 1 choroidal neovascularization lesion size: indocyanine green angiography versus optical coherence tomography angiography. *Invest Ophthalmol Vis Sci*. 2016;57:307–313.
31. Roisman L, Zhang Q, Wang RK, et al. Optical coherence tomography angiography of asymptomatic neovascularization in intermediate age-related macular degeneration. *Ophthalmology*. 2016;123:1309–1319.
32. Miller AR, Roisman L, Zhang Q, et al. Comparison between spectral-domain and swept-source optical coherence tomography angiographic imaging of choroidal neovascularization. *Invest Ophthalmol Vis Sci*. 2017;58:1499–1505.
33. Spaide RF. Optical coherence tomography angiography signs of vascular abnormalization with antiangiogenic therapy for choroidal neovascularization. *Am J Ophthalmol*. 2015;160:6–16.
34. Muakkassa NW, Chin AT, de Carlo T, et al. Characterizing the effect of anti-vascular endothelial growth factor therapy on treatment-naïve choroidal neovascularization using optical coherence tomography angiography. *Retina*. 2015;35:2252–2259.

Investigative Ophthalmology & Visual Science